PERGAMON

Journal of Structural Geology 22 (2000) 1621–1632

JOURNAL OF STRUCTURAL GEOLOGY

www.elsevier.nl/locate/jstrugeo

Microstructure and texture formation in extruded lead sulfide (galena)

Werner Skrotzki[a,*], Roland Tamm[a], Carl-Georg Oertel[a], Jens Röseberg[a], Heinz-Günter Brokmeier[b]

[a]*Institut für Kristallographie und Festkörperphysik, Technische Universität Dresden, D-01062 Dresden, Germany*
[b]*GKSS-Forschungszentrum Geesthacht GmbH, Max-Planck-Straße, D-21502 Geesthacht, Germany*

Received 25 November 1999; accepted 25 May 2000

Abstract

Lead sulfide (galena) of different purity and grain size was extruded through a round and rectangular die at temperatures between 773 and 923 K. Global and local lattice preferred orientations (here referred to as textures) were measured by neutron and electron back-scattering diffraction. Tension leads to a <100> <111> double fibre texture. Pure shear deformation yields texture components near the ideal face-centered cubic metal brass, copper, Goss and cube positions. The intensity of the components depends on the purity and/or grain size. The microstructure is partially recrystallized. Electron back-scattering diffraction indicates that in tension the <100 > and in pure shear the Goss and cube components are associated with dynamic recrystallization. The deformation texture can be qualitatively explained by the full and relaxed constraints Taylor model using slip on {100}<110>, {110}<110> and {111}<110> systems. The texture formation in lead sulfide compares well with that observed for other ionic crystals with the NaCl-structure as well as for face-centered cubic metals with a high stacking fault energy.

1. Introduction

Similar to other ionic crystals with the rock salt structure, PbS (galena) deforms by slip on {100}, {110} and {111} planes in <110> direction (Urusovskaya et al., 1964, 1978; Lyall and Paterson, 1966; McClay and Atkinson, 1977; Barthel, 1984; Foitzik et al., 1990, 1991). The critical resolved shear stresses (CRSS) for the activation of these slip systems are different. This plastic anisotropy depends on aliovalent doping, temperature, strain rate and ionicity of the material (Skrotzki and Haasen, 1981). For PbS at low temperatures {100} is the primary slip plane (Fig. 1, Barthel, 1984).

There exist six crystallographically equivalent {100}<110>, six {110}<110> and 12 {111}<110> slip systems. However, only two, three and five are independent, respectively. Thus, according to the von Mises criterion (von Mises, 1928), which requires five independent slip systems, slip on the harder secondary systems has to be activated simultaneously in order to deform a polycrystalline aggregate homogeneously. This should lead to difficulties at low temperatures where the plastic anisotropy is high due to the high Peierls potential for secondary slip (Haasen, 1985; Haasen et al., 1985). Nethertheless, the temperature dependence of the yield stress of PbS polycrystals indicates that the activation of secondary slip systems is necessary (Fig. 1, Skrotzki et al., 1981). However, their number and contribution to strain is not clear. With increasing temperature the plastic anisotropy decreases. In addition, dynamic recovery by cross-slip and climb, as well as dynamic recrystallization, become operative (McClay and Atkinson, 1977; Cox, 1987).

It is the aim of this paper to extend basic texture research on materials with high plastic anisotropy, such as salt (Skrotzki and Welch, 1983; Skrotzki, 1994; Skrotzki et al., 1995a, 1998), to materials of the same structure type but having an inverse plastic anisotropy, i.e. a change in primary slip. In order to test models on texture formation the development of texture in polycrystalline PbS has been examined during deformation in tension and pure shear, i.e. deformation modes with axial and orthorhombic symmetry, respectively. The results will be compared with those previously obtained on highly ionic crystals, such as salt (Skrotzki, 1994; Skrotzki and Welch, 1983; Skrotzki et al., 1998), less ionic chalcogenides, such as PbSe, PbTe (Ohrt, 1968) as well as with face-centered cubic (fcc) metals with high stacking fault energy (sfe), such as aluminum (e.g. Mecking, 1985; Fels, 1996; Hühne, 1997; Hühne et al., 1997). Preliminary results have already been published

* Corresponding author.
E-mail address: werner.skrotzki@physik.tu-dresden.de (W. Skrotzki).

0191-8141/00/$ - see front matter
PII: S0191-8141(00)00070-5

Table 1
Powder and sample characteristics

	Synthetic PbS powder	
	Pure	Impure
Supplier	Aldrich Chemical Comp., Inc.	VEB Feinchemie Eisenach
Purity according to supplier	99.9% PbS Impurities (Cu, Ni, Bi, Ag, Ca) < 500 ppm	$> 95\%$ PbS
Particle size	< 44 μm	≈ 9 μm
	Natural PbS sample	
Deposit locality	Braubach, Germany	
Mean composition (Jansen et al., 1998)	$79.9 \pm 6.5\%$ PbS, $2.6 \pm 0.6\%$ sulfosalt, $17.5 \pm 6.0\%$ ganque and other minerals. Material contains visible inclusions up to 1 mm diameter	
Grain size	34 μm	

elsewhere (Skrotzki et al., 1995b; Röseberg, 1996). Moreover, conclusions will be drawn on the interpretation of textures in naturally deformed galena.

2. Experimental details

Extrusion was carried out on compacted powders of different purity and on natural samples. Powder and sample characteristics are listed in Table 1. The powder particle size distribution was measured with a laser-particle-sizer "analysette 22" (Fritsch GmbH). The powders were compacted to cylinders by uniaxial compression at room temperature. The pressure varied from 100 to 200 MPa depending on powder quantity. To diminish friction, zinc stearate was used for lubrication. The compacted powders had a density of 5.89 g/cm^3 (pure) and 4.13 g/cm^3 (impure) compared to 7.57 g/cm^3 for fully dense PbS.

The cylindrical samples (Ø 30 mm) were extruded at temperatures between 773 and 923 K (0.56–0.67 T_m, T_m = melting temperature). Extrusion was carried out through a round (Ø 9 mm) and rectangular die (15.7×8.1 mm^2) which approximates tension and pure shear. The reduction in cross-section was 91% (true strain 2.41) and 82% (true strain 1.72), respectively. Extrusion at elevated temperatures increased the density from 87.4% to 99.6% (pure) and 54.6% to 77.8% (impure). The extrusion rate was 0.05 to 0.1 mm/s, and the maximum pressure needed was up to 1 GPa depending on temperature and material (Fig. 2). To reduce cracking of the sample, friction was increased by using a length/diameter ratio of the die of about six (Ohrt, 1968). The quality of the extruded samples, which depends on temperature, is shown in Fig. 3.

The microstructure of the extruded rods was investigated in a scanning electron microscope (SEM, Zeiss DSM 962) with a four quadrant back-scattering detector. Transverse and longitudinal sections were cut with a diamond saw. They were polished mechanically on SiC grinding paper (grit 320–4000) and chemically with a solution of HCl, HNO_3, CH_3COOH (30:10:1) at 343 K for 30–60 s (Brebrick and Scanlon, 1957). Rinsing in 10% acetic acid removed the gray surface layer that formed. Grain boundaries were etched at 343 K for 20–60 s in a solution of thiourea (100 g/l) and HCl (3:1).

Complete pole figures for {200}, {220} and {111} reflections were measured by neutron diffraction at the GKSS Research Centre in Geesthacht, Germany. Orientation distribution functions (ODF) were calculated using the series expansion method up to a series expansion degree of 22 and axial or orthorhombic sample symmetry (Dahms, 1992; Dahms and Eschner, 1996). In addition, semiautomatic electron back-scattering diffraction (EBSD) measurements were carried out on a SEM (Zeiss DSM 962) in order to correlate the texture components with the microstructure shown by orientation contrast. The EBSD patterns were analysed with the software package Channel+ developed by HKL-Software, Hobro, Denmark.

The textures were simulated with the full and relaxed constraints Taylor model (FC and RC) (Taylor, 1938; van Houtte, 1988) by using 1003 orientations randomly distributed in the Euler space (Helming, 1997). The mean distance between neighbouring orientations was 9°. The strains relaxed were ε_{xz} and ε_{xy} (RC round die), ε_{xz} (RC 1 rectangular die) and ε_{xz} and ε_{yz} (RC 2 rectangular die) with x being the extrusion, y the transverse and z the normal direction (ED, TD, ND). In all simulations the total true strain was achieved in steps of 5%. The tensor describing the strain mode is approximated by

$$\begin{matrix} q\text{-}1 & 0 & 0 \\ 0 & -q & 0 \\ 0 & 0 & 1 \end{matrix}$$

with $q = \ln(a/d)/\ln(ha/d^2)$, d: initial diameter, a: long side of rectangular die, h: short side of rectangular die (Dahms,

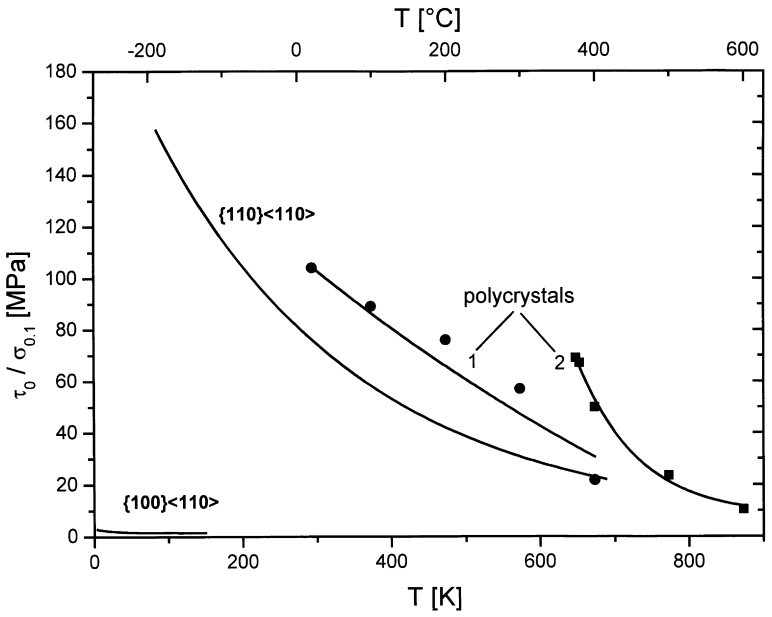

Fig. 1. Temperature dependence of the critical flow stress of PbS polycrystals taken at 0.1% strain (1: natural, p = 0.2–0.3 GPa, $\dot{\varepsilon} = 4.8 \cdot 10^{-5}$ s^{-1}, Jansen et al., 1998; 2: pure synthetic, $\dot{\varepsilon} = 10^{-4}$ s^{-1}) and the CRSS for {100}<110> and {110}<110> slip of single crystals (Barthel, 1984, $\dot{\varepsilon} = 10^{-4}$ s^{-1}).

private communication). $q = 0.5$ describes tension, $q = 0.0$ plane strain and values between pure shear. For extrusion through the rectangular die used, $q = 0.33$. However, it should be noted that so far the limitations of this approximation have not been checked by finite element calculations. The slip systems used were {100}<110>, {110}<110> and {111}<110>; their relative CRSS chosen were 1:5:5 and 1:1:1, reflecting deformation at medium to high temperatures (Fig. 1).

3. Results

Tension of impure PbS between 773 and 923 K leads to a weak <111> fibre texture. In contrast, pure and natural PbS exhibit a pronounced <111> <100> double fibre texture (Fig. 4). The difference depends on purity and/or grain size. In the temperature range investigated the intensity of the <111> fibre has a maximum at about 873 K, where <100> is strongest. Pure shear yields maxima near the

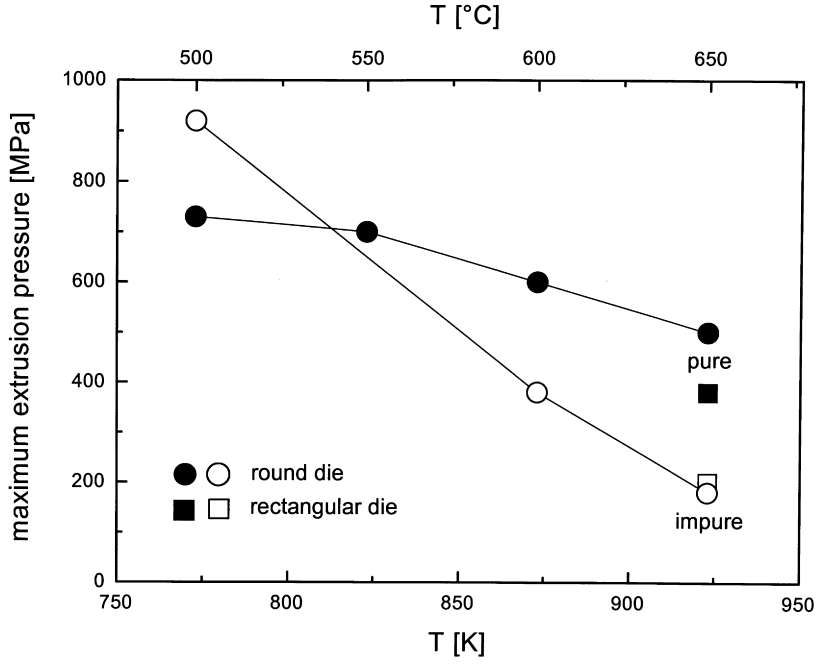

Fig. 2. Temperature dependence of the maximum extrusion pressure for pure and impure PbS.

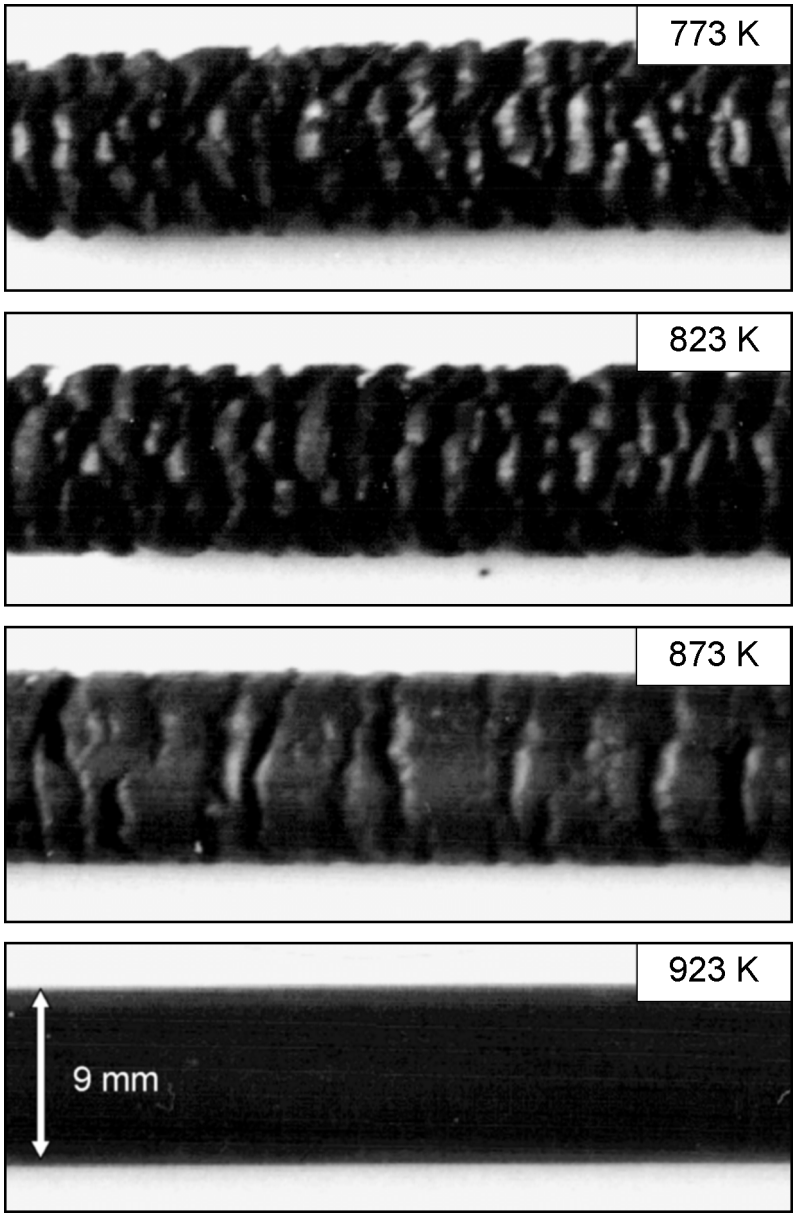

Fig. 3. Photographs of the extruded pure PbS rods showing an increase of cracking at the surface with decreasing temperature.

brass (Bs: {110}<112>), copper (Cu: {112}<111>), cube (C: {100}<100>), and Goss (G: {110}<100>) ideal components generally observed in fcc metals (Fig. 5). However, these components are only clearly seen in the pure material, and weakly indicated in the natural material. Both the impure and the natural sample have a very weak texture, with the texture of the impure PbS being almost random.

Selected EBSD measurements on the pure and natural samples indicate that the predominant <111> fibre and the Cu, Bs and G components exist in the deformed grains. The <100> fibre, C and G are mainly found in the recrystallized parts (Figs. 6 and 7). The deformed grains are highly elongated and have a subgrain structure, while the recrystallized areas are characterized by an equiaxed grain structure and high angle boundaries (Fig. 8). As the grain structure of the impure samples was too small to be resolved, EBSD measurements on this material could not be carrried out.

In tension all simulations yield the <111> fibre. With decreasing anisotropy a <100> fibre appears which becomes stronger by relaxation (Fig. 9). In pure shear the texture is more sensitive to the simulation model (Fig. 10). Here FC and RC 1 simulations for $q = 0.3$ yield components close to Cu and Bs. Decreasing the plastic anisotropy and introducing relaxation (RC 1) results in a weak C and Goss component. To give an impression of how the texture varies with q, for comparison plane strain deformation ($q = 0$) has

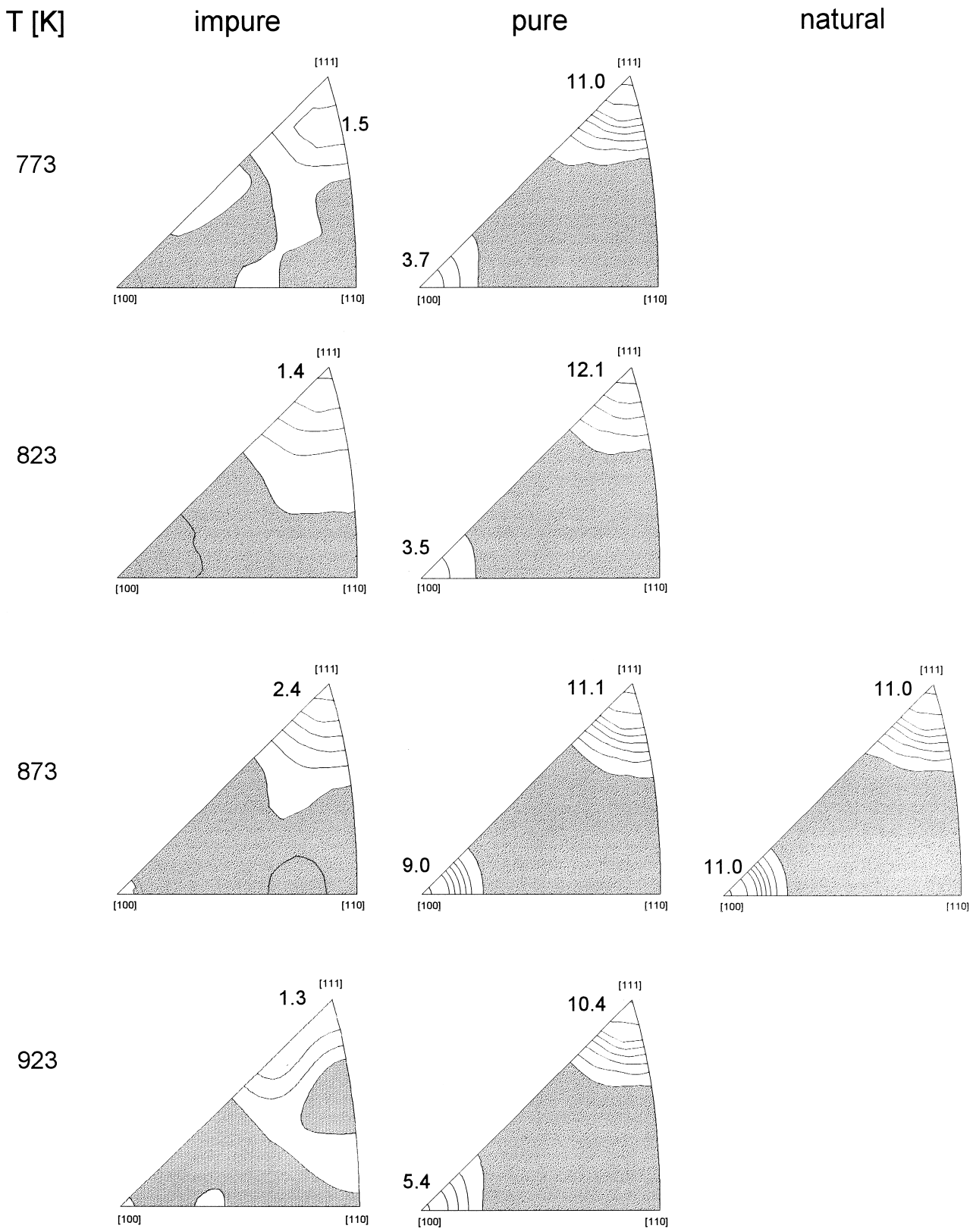

Fig. 4. Experimental PbS textures after extrusion through a round die ($q = 0.5$). Intensities of the inverse pole figures of the extrusion direction ED are given in multiples of a random distribution; the area below unity is shaded.

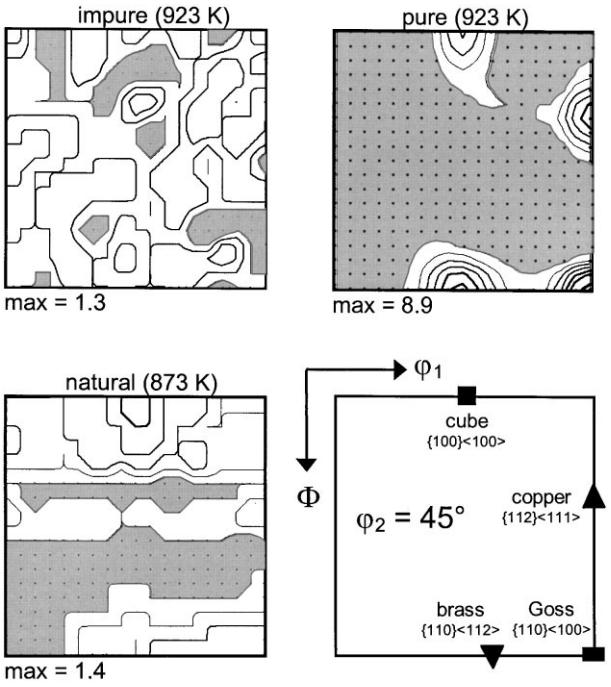

Fig. 5. Experimental PbS textures ($\varphi_2 = 45°$ ODF sections) after extrusion through a rectangular die.

also been simulated. Beside the Cu component this deformation mode leads to an incomplete {110}<uvw> fibre (intensity along lower line in $\varphi_2 = 45°$ ODF section). In addition, for plastic isotropy and relaxation a weak C appears. RC 2 in all simulations considered leads to a strong component close to Cu.

4. Discussion

Because of their low-temperature brittleness, PbS polycrystals can only be extruded above 773 K at the deformation rate used. For lead chalcogenides the critical temperature decreases with increasing contribution of metallic bonding (Ohrt, 1968): PbSe 636 K, PbTe 417 K. The textures obtained in axial extrusion for these lead chalcogenides are <111> <100> double fibre textures. However, as microstructural studies are missing it is left open whether recrystallization has also occurred. Textures at lower temperatures have only been reported for natural PbS deformed in compression under confining pressure (Siemes, 1976, 1977; Siemes and Hennig-Michaeli, 1985; Martens, 1987; Siemes et al., 1994; Jansen et al., 1998). The textures observed after deformation between 573 and 773 K are <110> fibre textures. Recrystallization of samples compressed at room temperature led to a randomization of the texture (Siemes, 1976, 1977). The textures of PbS presented here for deformation with orthorhombic symmetry are the first reported so far.

Texture formation is affected by purity and grain size of the material. Impurities suppress recrystallization by hindering grain boundary migration, while decreasing grain size leads to homogeneous deformation. Moreover, below a certain grain size the contribution to strain of grain boundary sliding increases strongly (Nieh et al., 1997). These arguments may explain the different texture evolution in pure and impure PbS. Owing to a lower grain size of the impure PbS grain boundary sliding could contribute to strain and reduce texture formation. On the other hand less slip activity leads to a lower stored energy preventing the onset of recrystallization. Moreover, recrystallization may also be suppressed by the impurities. The contribution of grain boundary sliding may also explain the lower extrusion pressure at high temperatures needed for impure PbS (Fig. 2). The strong variation in strength of texture of natural samples may be due to a large composition variation within the sample suite.

The deformation textures have been simulated with the Taylor theory. As the input parameters are not known well enough for the materials investigated, different sets of parameters have been used to model the textural trend observed with temperature. Increasing temperature leads to a decreasing plastic anisotropy. Diffusional processes become important, accommodating incompatibilities arising from inhomogeneous slip within the grains. This effect has been accounted for by relaxation, which becomes more important as the grain shape becomes more and more distorted with deformation. Therefore, according to Hosford (1993) the volume fractions of the material requiring 3, 4 and 5 independent slip systems should have been changed with strain. The comparison between experimental and simulated textures shows that the textural trend with temperature for tension ($q = 0.0$) and pure shear ($q = 0.3$) is well described by a decreasing plastic anisotropy, as well as by some degree of relaxation. Unfortunately, the comparison is only qualitative because of the arguments given above and because it is not known to what extent the volume fractions of the components have been changed by recrystallization. The <100>, C and G deformation components seem to be the nuclei for recrystallization, similar to fcc metals (Humphreys and Hatherly, 1995). It should be noted that the low-temperature compression textures mentioned above can also be modelled well with the FC Taylor theory, the result being quite independent of the plastic anisotropy used. This is in agreement with previous simulations by Siemes (1965, 1974).

The textures observed are comparable with those generally observed in highly ionic crystals with inverse plastic anisotropy, as well as in fcc metals with high stacking fault energy primarily gliding on {111} (Skrotzki et al., 1995a, 1998; Hühne et al., 1997; Fig. 11). The comparison of NaCl-type ionic crystals of different ionicity, i.e. different plastic anisotropy, with high sfe fcc metals clearly shows that texture development during high strain deformation does not strongly depend on the plastic anisotropy existing at the onset of deformation of single crystals. High strain deformation at elevated temperatures is dominated by

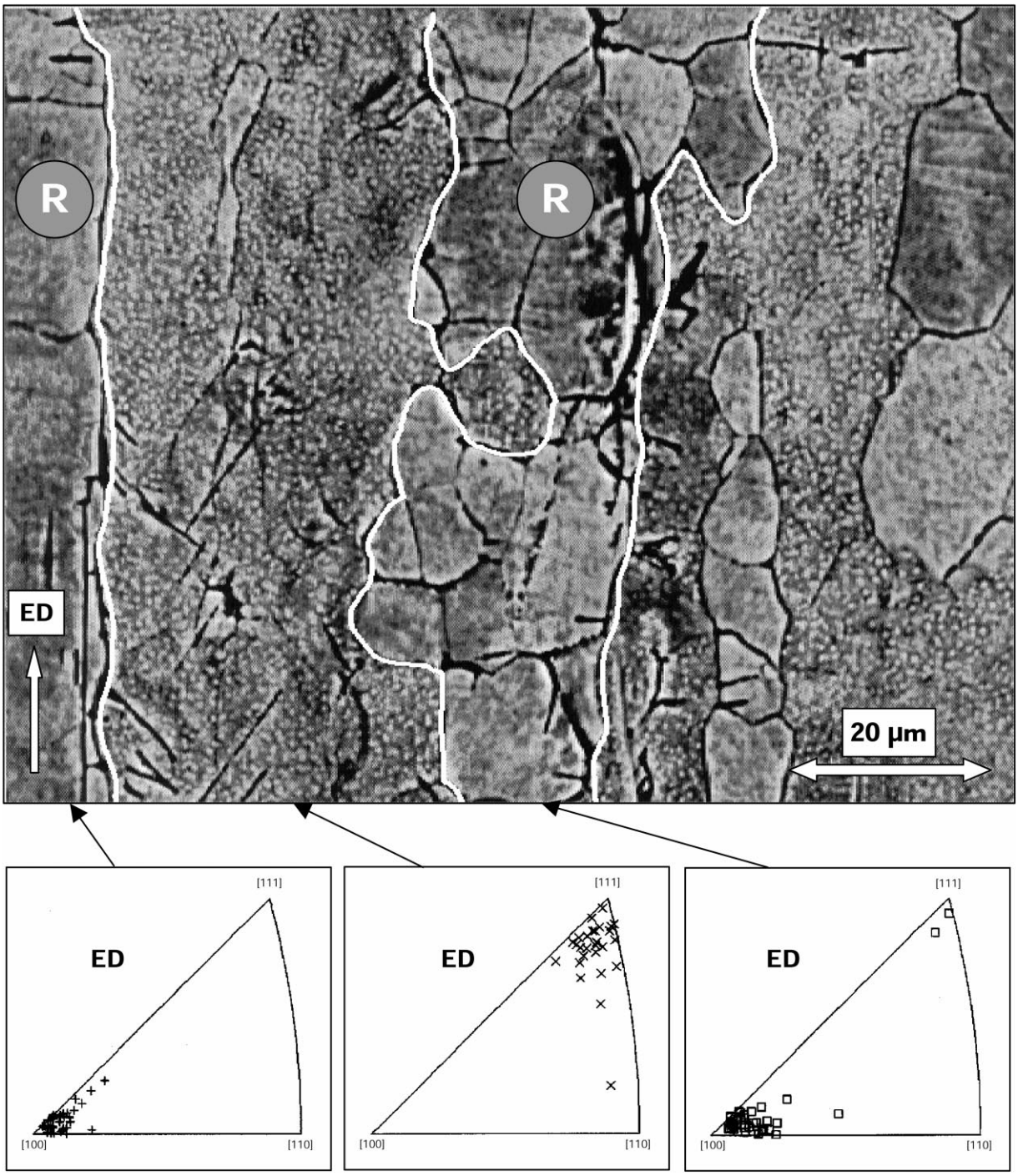

Fig. 6. Microstructure (orientation contrast image) and texture (EBSD measurements) of different regions in a natural PbS sample extruded through a round die at 873 K. Elongated deformed and recrystallized (R) areas selected for EBSD measurements are separated by white lines. ED = extrusion direction.

cross-slip, i.e. the main slip parameter seems to be the Burgers vector, and this is the same for NaCl-type ionic crystals and fcc metals.

Galena deposited in veins is often naturally deformed by postdepositional tectonic processes. The deformation may change the coarse protogranular grain structure to a fine or even ultrafine mylonitic grain structure with a well-defined foliation *S* more or less parallel to the macroscopic shear plane and a lineation *L*, which is the mineral elongation direction contained in the foliation (McClay, 1982). Correspondingly, textures from different locations show considerable variation. A <100> fibre texture with the fibre axis aligned normal to the vein wall has been described by Schachner-Korn (1954) as growth texture. In general,

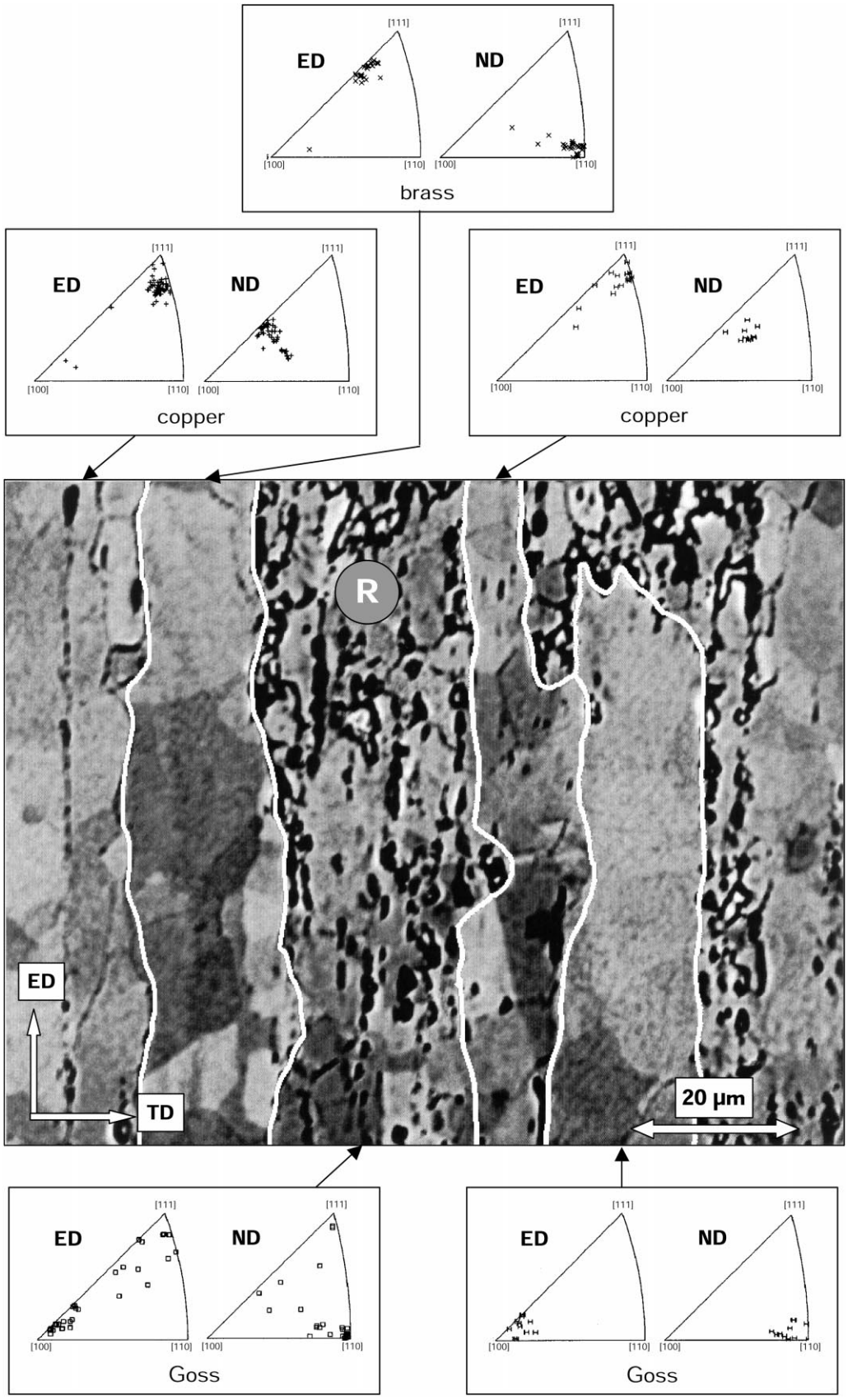

Fig. 7. Microstructure (orientation contrast image) and texture (EBSD measurements) of different regions in a pure PbS sample extruded through a rectangular die at 923 K. Elongated deformed and recrystallized (R) areas selected for EBSD measurements are separated by white lines. ED = extrusion direction; ND = normal direction.

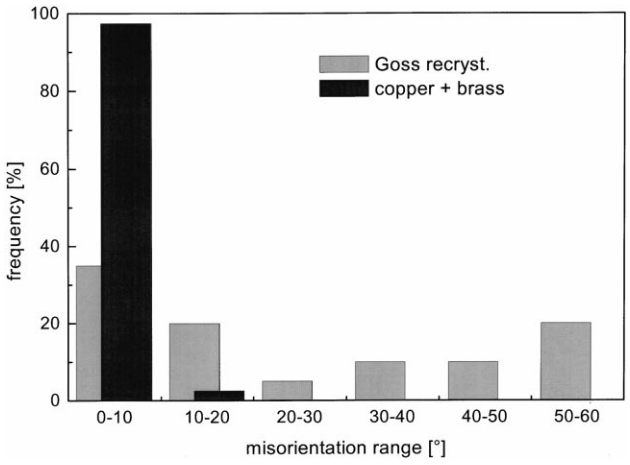

Fig. 8. Frequency of misorientation angles of grain boundaries in deformed (Cu and Bs) and recrystallized (G) regions in a pure PbS sample extruded through a rectangular die at 923 K.

deformation textures have been reported, which may be classified in two groups (McClay, 1980, 1983; Siemes and Spangenberg, 1980). The first has a dominant Cu component, with {112} ∥ S and <111> ∥ L. The second consists of a dominant 45° rotated cube component, with {100} ∥ S and <110> ∥ L, and a superimposed incomplete <110> fibre texture, with {100} to {111} ∥ S and <110> ∥ L. These textures may have been produced by pure and simple shear deformation, respectively. They can be simulated with the FC Taylor theory (Fig. 10, $q = 0.0$; Siemes and Schachner-Korn 1965; Siemes and Spangenberg, 1980). This interpretation implies that the recrystallization process did not change the deformation texture, which may only be the case for a rotation recrystallization mechanism. Support for such a mechanism is given by the upper deformation temperature estimated (200°C, McClay, 1980). In contrast, in the present work recrystallization took place at higher temperatures by a migration mechanism. Thus, selected grain growth of minor components of the deformation texture may dominate the recrystallization texture. Moreover, relaxation leads to further deformation components, like the Bs component in plane strain. If natural deformation by dynamic recrystallization produces an ultrafine grain structure, then Coble creep or superplastic deformation does not lead to any preferred orientation (McClay, 1980, 1983). This is in agreement with present observations on fine-grained impure PbS.

5. Conclusions

1. Tension of PbS above 773 K leads to a <111> <100> double fibre texture. Pure shear deformation yields components near the ideal fcc metal copper, brass, Goss and cube positions. The intensity of the components depends on the purity and/or grain size.
2. The <100> fibre, cube and Goss components are associated with dynamic recrystallization.
3. The deformation texture can be qualitatively explained by the full and relaxed constraints Taylor model using slip on {100}<110>, {110}<110> and {111}<110> systems.
4. The texture formation in PbS compares well with that observed for other ionic crystals with inverse plastic anisotropy as well as for fcc metals with high stacking fault energy.
5. Textures of naturally deformed galena can be interpreted by pure and simple shear deformation. However, this implies that recrystallization has taken place by a rotation mechanism and therefore did not change the deformation texture.

Acknowledgements

Thanks are due to the Deutsche Forschungsgemeinschaft for financial support through grants Sk 21/7-1 (W.S.) and Ho 1342/5-1 (R.T.). The extrusions were carried out by R. Opitz, IFW Dresden. The textures were simulated with the computer program developed by Prof. P. van Houtte. The natural samples were kindly provided by Dr E.M. Jansen.

References

Barthel, C., 1984. Plastische Anisotropie von Bleisulfid und Magnesiumoxid. Diploma thesis, University of Göttingen.

Brebrick, R.F., Scanlon, W.W., 1957. Chemical etches and etch pit patterns on PbS crystals. Journal of Chemistry and Physics 27, 607–608.

Cox, S.F., 1987. Flow mechanisms in sulphide minerals. Ore Geological Review 2, 133–171.

Dahms, M., 1992. The iterative series expansion method for quantitative texture analysis—Part II: Applications. Journal of Applied Crystallography 25, 258–267.

Dahms, M., Eschner, T., 1996. Quantitative Texturanalyse durch iterative Reihenzerlegung von Beugungspolfiguren. Software manual.

Fels, B., 1996. Textur- und Mikrostrukturuntersuchungen an strangepreßtem Aluminium. Diploma thesis, Dresden University of Technology.

Foitzik, A., Skrotzki, W., Haasen, P., 1990. Dislocation microstructure on {100} and {110} slip planes in lead sulphide. Physica Status Solidi (a) 121, 81–94.

Foitzik, A., Skrotzki, W., Haasen, P., 1991. Slip on {111} planes in lead sulphide. Materials Science and Engineering A132, 77–82.

Haasen, P., 1985. Dislocations and the plasticity of ionic crystals. Materials Science and Technology 1, 1013–1024.

Haasen, P., Barthel, C., Suzuki, T., 1985. Choice of slip system and Peierls stresses in the NaCl structure, Yamada Science Foundation, University of Tokyo Press, Tokyo, pp. 455–461.

Helming, K., 1997. A nearly equal distant grid of orientations for quantitative texture analysis. Textures and Microstructures 28, 219–230.

Hosford, W.F., 1993. The Mechanics of Crystals and Textured Polycrystals. Oxford University Press, Oxford.

Hühne, R., 1997. Untersuchung der Entstehung von Rekristallisationstexturen in Al-Legierungen. Diploma thesis, Dresden University of Technology.

Hühne, R., Fels, B., Tamm, R., Oertel, C.-G., Skrotzki, W., 1997. Cube texture formation in a rectangular die extruded Al-Mg alloy. Proceedings International Conference on Texture and Anisotropy of

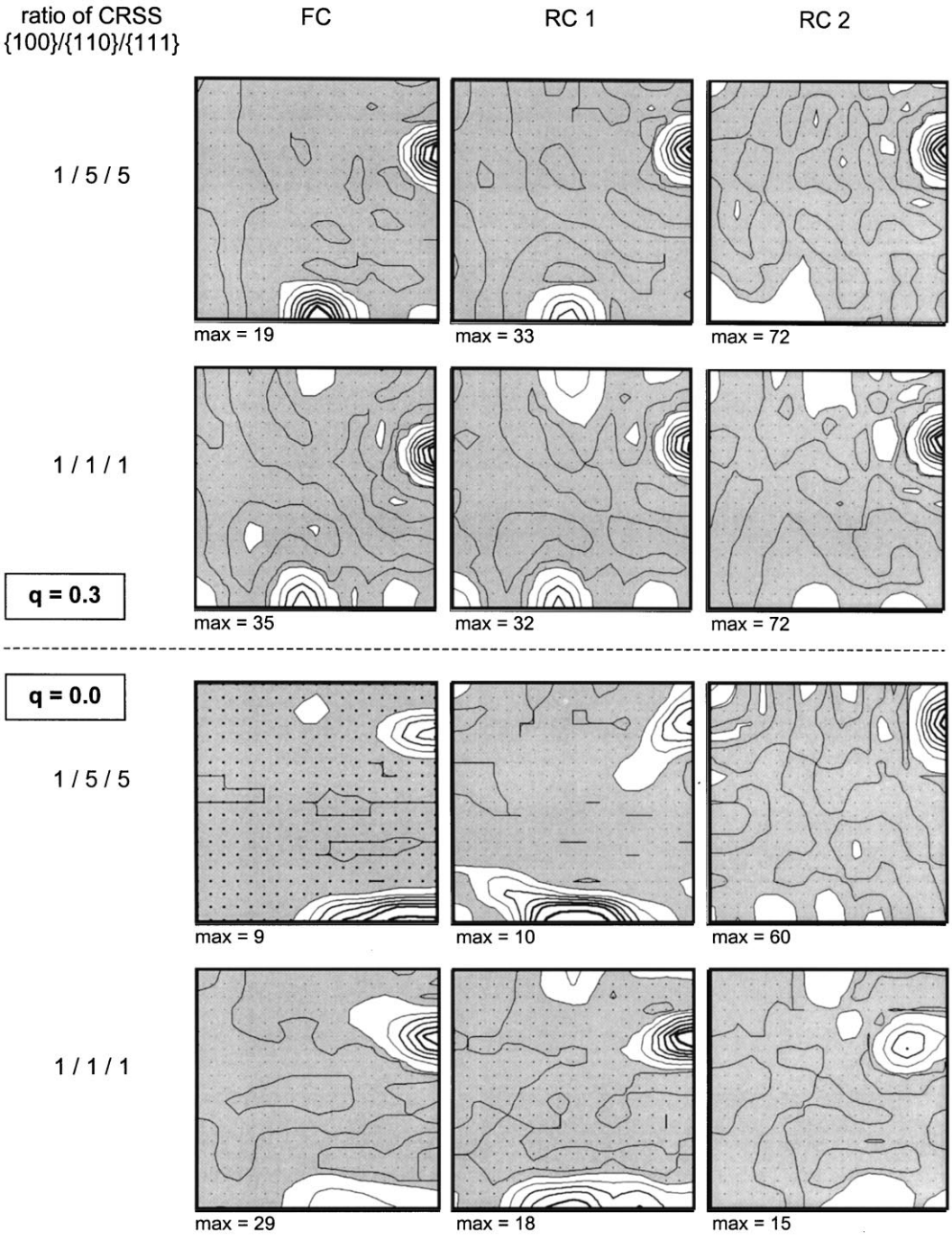

Fig. 9. Textures simulated for tension ($q = 0.5$, inverse pole figures of the extrusion direction ED).

Polycrystals, Clausthal. Trans Tech Publications, Switzerland, pp. 471–476.

Humphreys, F.J., Hatherly, M., 1995. Recrystallization and Related Annealing Phenomena. Pergamon Press, Oxford.

Jansen, E.M., Siemes, H., Brokmeier, H.-G., 1998. Crystallographic preferred orientation and microstructure of experimentally deformed Braubach galena ore with emphasis on the relation to diffusional processes. Mineralium Deposita 34, 57–70.

Lyall, K.D., Paterson, M.S., 1966. Plastic deformation of galena (lead sulphide). Acta Metallurgica 14, 371–383.

Martens, L., 1987. Verformbarkeit und Regelung von Galenit und Sphalerit in Mischerzen in Abhängigkeit von der Zusammensetzung, der Verformungstemperatur und der Verformungsrate. Ph.D. thesis, RWTH Aachen.

McClay, K.R., Atkinson, B.K., 1977. Experimentally induced kinking and annealing of single crystals of galena. Tectonophysics 39, 175–189.

McClay, K.R., 1980. Sheared galena; textures and microstructures. Journal of Structural Geology 2, 227–234.

McClay, K.R., 1982. Fabrics in ores. In: Borradaile, G.J., Bayly, M.B., Powell (Eds.). Atlas of Deformational and Metamorphic Rock Fabrics. Springer, Berlin, pp. 374–383.

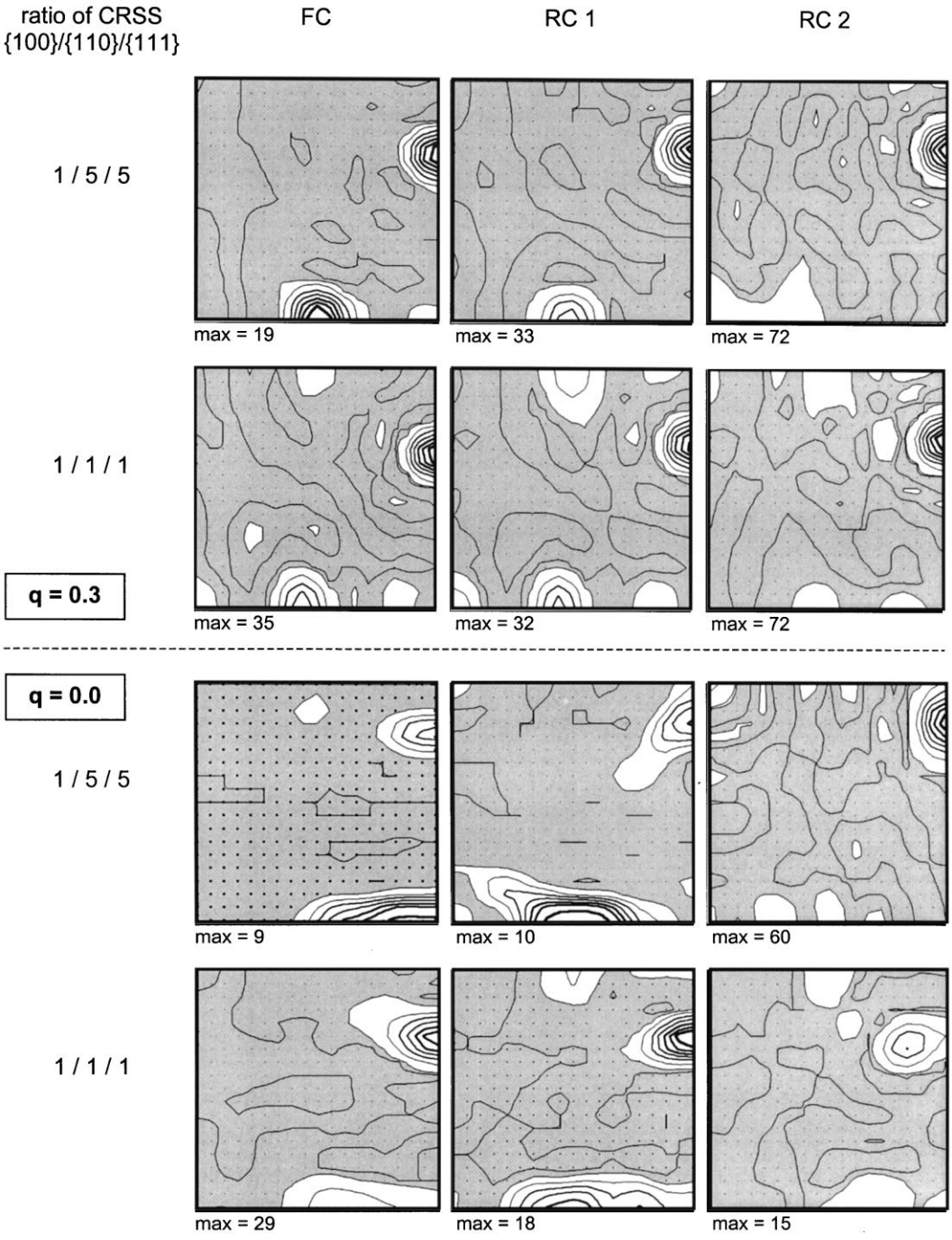

Fig. 10. Textures ($\varphi_2 = 45°$ ODF sections) simulated for pure shear ($q = 0.3$) and plane strain ($q = 0.0$) deformation.

McClay, K.R., 1983. Fabrics of deformed sulphides. Geologische Rundschau 72, 469–491.

Mecking, H., 1985. Textures in metals. In: Wenk, H.-R. (Ed.). Preferred Orientation in Deformed Metals and Rocks: An Introduction to Modern Texture Analysis. Academic Press, New York, pp. 267–306.

Nieh, T.G., Wadsworth, J., Sherby, O.D., 1997. Superplasticity in Metals and Ceramics. Cambridge University Press, Cambridge.

Ohrt, E., 1968. Über das Strangpressen intermetallischer Verbindungen. Bänder Bleche Rohre 9, 327–331.

Röseberg, J., 1996. Textur- und Mikrostrukturuntersuchungen an verformten PbS-Polykristallen. Diploma thesis, Dresden University of Technology.

Schachner-Korn, D., 1954. Ein Wachstums- und ein Rekristallisationsgefüge von Bleiglanz aus einer rheinischen Lagerstätte. Tschermaks Mineralogische und Petrographische Mitteilungen 4, 111–116.

Siemes, H., 1965. Theoretische Ableitung der Stauchtexturen von Bleiglanz. Neues Jahrbuch für Mineralogie. Abhandlungen 103, 80–93.

Siemes, H., 1974. Anwendung der Taylor-Theorie auf die Regelung von kubischen Mineralen. Contributions to Mineralogy and Petrology 43, 149–157.

Siemes, H., 1976. Recovery and recrystallization of experimentally deformed galena. Economic Geology 71, 763–771.

Siemes, H., 1977. Recovery and recrystallization of deformed galena. Tectonophysics 39, 171–174.

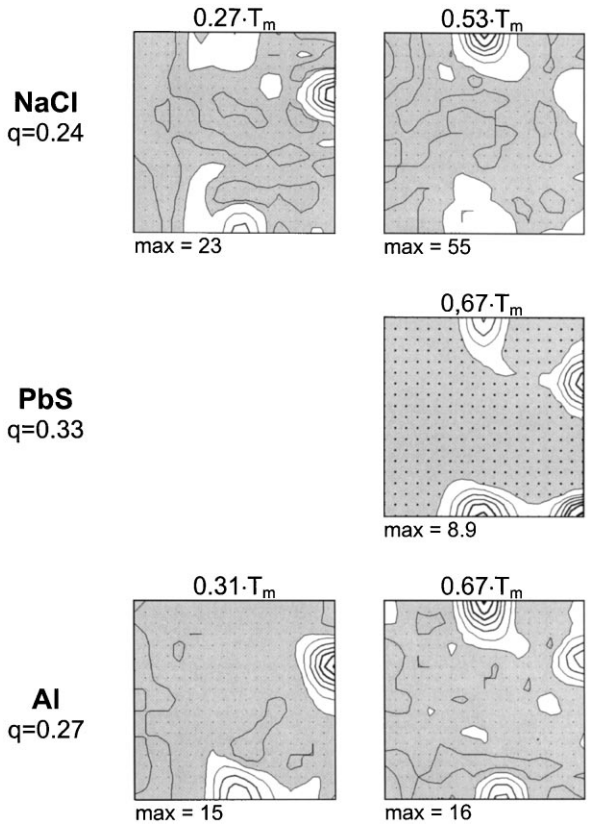

Fig. 11. Comparison of textures ($\varphi_2 = 45°$ ODF sections) for PbS, NaCl and Al extruded through a rectangular die. (NaCl: Skrotzki et al., 1995, Al: Hühne et al., 1997)

Siemes, H., Schachner-Korn, D., 1965. Theoretische Ableitung der Schertexturen von Bleiglanz und Vergleich dieser mit Texturen natürlich verformter Bleiglanze. Neues Jahrbuch für Mineralogie. Abhandlungen 102, 221–250.

Siemes, H., Spangenberg, H.J., 1980. Shear fabrics of naturally deformed galena. Journal of Structural Geology 2, 235–241.

Siemes, H., Hennig-Michaeli, Ch., 1985. Ore minerals. In: Wenk, H.-R. (Ed.). Preferred Orientation in Deformed Metals and Rocks: An Introduction to Modern Texture Analysis. Academic Press, New York, pp. 335–360.

Siemes, H., Jansen, E.M., Niederschlag, E., 1994. Crystallographic preferred orientations of experimentally deformed sulfide ores. In: Bunge, H.J., Siegesmund, S., Skrotzki, W., Weber, K. (Eds.). Textures of Geological Materials. DGM Informationsgesellschaft Verlag, Oberursel, pp. 231–250.

Skrotzki, W., 1994. Mechanisms of texture development in rocks. In: Bunge, H.J., Siegesmund, S., Skrotzki, W., Weber, K. (Eds.). Textures of Geological Materials. DGM Informationsgesellschaft Verlag, Oberursel, pp. 167–187.

Skrotzki, W., Haasen, P., 1981. Hardening mechanisms of ionic crystals on (110) and (100) slip planes. Journal de Physique 42, 119–148.

Skrotzki, W., Welch, P., 1983. Development of texture and microstructure in extruded ionic polycrystalline aggregates. Tectonophysics 99, 46–47.

Skrotzki, W., Frommeyer, G., Haasen, P., 1981. Plasticity of polycrystalline ionic solids. Physica Status Solidi (a) 66, 219–228.

Skrotzki, W., Helming, K., Brokmeier, H.-G., Dornbusch, H.-J., Welch, P., 1995a. Textures in pure shear deformed rock salt. Textures and Microstructures 24, 133–141.

Skrotzki, W., Helming, K., Oertel, C.-G., Röseberg, J., Tamm, R., Brokmeier, H.-G., 1995b. Textures in extruded lead sulfide. Proceedings of the 11th International Conference on Textures of Materials, Xian, pp. 1039–1044.

Skrotzki, W., Dornbusch, H.-J., Helming, K., Tamm, R., Brokmeier, H.-G., 1998. Development of microstructure and texture in pure shear deformed salt. Series on Rock and Soil Mechanics 22, 101–114.

Taylor, G.I., 1938. Plastic strain in metals. Journal of the Institute of Metals 62, 307–324.

Urusovskaya, A.A., Tyaagaradzhan, R., Klassen-Neklyudova, M.V., 1964. Dislocation structure in PbS crystals in the range of concentrated load. Soviet Physics—Crystallography 8, 501–505.

Urusovskaya, A.A., Sizova, N.L., Sangwal, K., Smirnov, S.P., 1978. Plastic deformation of PbS crystals on compression along the <100> direction. Soviet Physics Solid State 20, 835–836.

van Houtte, P., 1988. A comprehensive mathematical formulation of an extended Taylor-Bishop-Hill model featuring relaxed constraints, the Renouard-Wintenberger theory and strain rate sensitivity model. Textures and Microstructures 8-9, 313–350.

von Mises, R., 1928. Mechanik der plastischen Formänderung von Kristallen. Zeitschrift für Angewandte und Mathematische Mechanik 8, 161–185.